Application of a Model-Based Flight Director Design Technique to a Longitudinal Hover Task

Ronald A. Hess*
NASA Ames Research Center, Moffett Field, Calif.

sAn analytical pilot model is used to design flight director laws for longitudinal control of a UH-1H helicopter in hovering flight in the presence of longitudinal turbulence. A simplified design technique is demonstrated which uses only essential feedbacks in synthesizing the director laws. The flight director is evaluated in a fixed-based pilot-in-the-loop simulation, in which root mean square performance and pilot opinion ratings are obtained. Significant improvement in performance and pilot ratings is achieved with the director as compared to the baseline display, in which only status information is presented. Based upon simulation results, the pilot model is refined, and improved director laws are generated and analytically evaluated using the refined model.

I. Introduction

A. Background

A FLIGHT director system is one in which the various displayed and/or sensed variables used by the pilot in performing a given task are combined into one instrument, forming a single-loop compensatory tracking task for each of the controls available to the pilot. The flight director, and the "laws" that govern the movement of the display elements that constitute the director can reduce the pilot's workload significantly. In certain situations, such as V/STOL approach and landing tasks, a well-designed director can be a necessity.

The flight director design problem obviously centers about determining the director laws, i.e., finding the appropriate mix of vehicle motion quantities to drive the director display elements. As pointed out in Ref. 1, this mix historically has been determined by 1) adapting and displaying the output of an automatic flight control system, or 2) choosing appropriate vehicle motion quantities based upon guidance and control requirements. Neither of these approaches explicitly considers the pilot-centered characteristics until the system is simulated or flight tested. The work of Ref. 1 considers the use of classical frequency domain representations of the human pilot in director design problems. Reference 2 suggests a director design procedure using the optimal pilot model. Both techniques offer considerable improvement over the design procedures 1 and 2, since pilot characteristics are considered at the design stage.

In the research to be described, a simplified director design technique, which uses the optimal pilot model, is employed. Only essential feedbacks are used in the director laws. Specifically, the optimal pilot model is used to design a director of minimum complexity for longitudinal control of a UH-1H helicopter in hovering flight in the presence of longitudinal turbulence. The director is evaluated in a fixed-base pilot-in-the-loop simulation, and on the basis of simulation results, modifications are discussed.

B. Vehicle/Task Description

The aerodynamic data for the UH-1H helicopter are shown in Table 1. The data are for hovering flight out of ground effect. The vehicle possesses a stabilizer bar (a device attached to the rotor hub providing pitch and roll damping), but no other stability augmentation system. The inclusion of a propertly designed stability augmentation system normally would be a prerequisite for an instrument hover in a vehicle such as this. However, in order to ascertain the benefits to be accrued from display improvement alone, no augmentation was used. Figure 1 shows the display symbology. The display is "head-down" in nature, and consists of a stroke-written cathode-ray-tube (CRT). In the baseline configuration, the director symbology is removed; in the director configuration, it is retained. The turbulence spectrum is shown in Table 2. Only longitudinal motion is considered. The pilot's task consists of maintaining the vehicle over the center of a landing pad 15.2 m (50 ft) on a side and at a reference height. The actual value of the reference height is not pertinent, except that the vehicle is out of ground effect. The pilot has two controls, longitudinal cyclic pitch and collective pitch. On the UH-1H vehicle, rotor rpm is held constant through the action of a power governor.

C. Analytical/Experimental Approach

The analytical flight director design technique to be used is based upon that offered in Ref. 2. As employed here, the technique is a logical extension of the work of Ref. 3, in which display quickening laws were derived for another helicopter in landing approach. The experimental work consisted of a fixed-base simulation to be described.

II. Optimal Pilot Model

A. Introduction

A detailed description of the optimal pilot model is beyond the scope of this paper. The reader is instead referred to Ref. 4

Table 1 Normalized UH-1H longitudinal derivatives in stability axis system, hover

m	$=3{,}856$ kg	M_u	$=0.00314$/sec-m
U_0	$=0$ m/sec	M_w	$=-.00477$ /sec-m
I_{yy}	$=17{,}279$ kg-sec^2	$M_{\dot{w}}$	$=0$/m
X_u	$=-0.00934$ /sec[a]	M_q	$=-2.03$ /sec
X_w	$=-0.000418$ /sec	X_{δ_B}	$=12.5$ /sec^2
X_q	$=5.88$ m/sec	X_{δ_C}	$=0.00187$ /sec^2
Z_u	$=-0.00214$ /sec	Z_{δ_B}	$=-0.308$ /sec^2
Z_w	$=-0.404$ /sec	Z_{δ_C}	$=-96.1$ /sec^2
Z_q	$=0.462$ m/sec	M_{δ_B}	$=-4.20$ /m-sec^2
		M_{δ_C}	$=0$ /m-sec^2

[a]Force and moment derivatives are normalized with respect to mass and moment of inertia, e.g., $X_u = 1/m)\,(\partial X/\partial u)_0$; $M_u = 1/I_{yy})\,(\partial M/\partial u)_0$.

Received Feb. 26, 1976; revision received Sept. 13, 1976.
Index categories: VTOL Handling, Stability, and Control; Navigation, Control, and Guidance Theory.

*Assistant Professor, Dept. of Aeronautics, Naval Postgraduate School, Monterey, California. On assignment at Ames Research Center, NASA. Member AIAA.

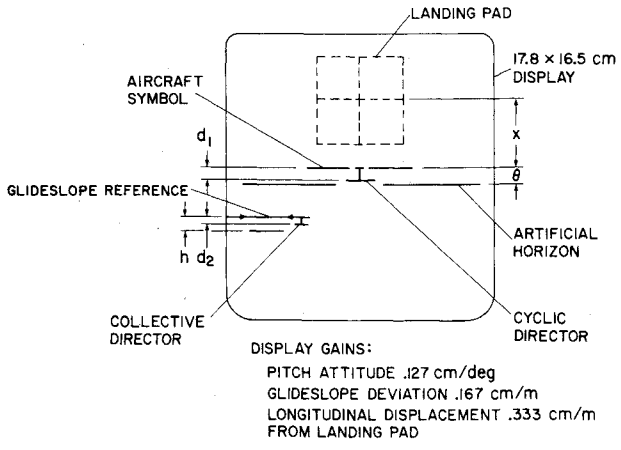

Fig. 1 CRT display for UH-1H hover.

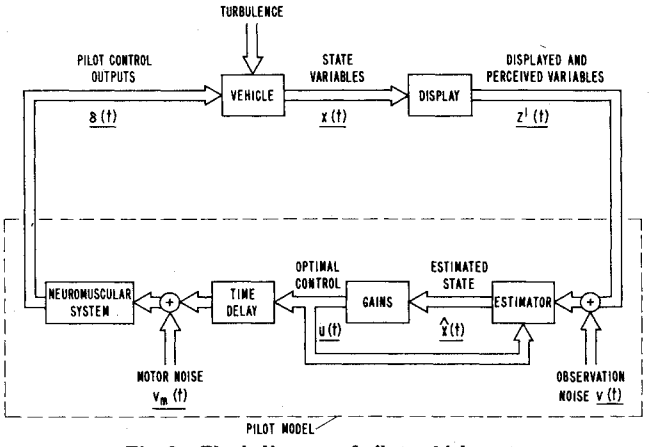

Fig. 2 Block diagram of pilot-vehicle system.

Table 2 Turbulence spectrum for UH-1H hover

$$\Phi_{u_g u_g}(\omega) = \frac{2\sigma^2_{u_g} L_u}{U_0} \quad \frac{1}{1+(L_u\omega/U_0)^2} \text{ m}^2\text{rad/sec}^2$$

$$\sigma_{u_g} = 1.52 \text{ m/sec (5 fps)}$$

$$L_u/U_0 = 3.33 \text{ sec}^a$$

[a] Although $U_0 = 0$ and the "frozen turbulence" hypothesis is, strictly speaking, no longer valid, the general form of the turbulence spectrum mentioned previously is retained. For example, one can consider $U_0 = 1.52$ m/sec, $L_u = 5.06$ m.

for specifics. The basic hypothesis behind the model can be given as follows: Subject to his inherent limitations, the well-trained, well-motivated pilot behaves in an optimal manner. The pilot's control characteristics can be modeled by the solution of an optimal linear control and estimation problem with certain specifications. As used in this study, these specifications can be summarized as follows:

1) Time delay – A pure time delay is included in each of the pilot's control outputs.

2) Neuromuscular dynamics – Each output neuromuscular system is modeled as a first-order lag, or, equivalently, control *rate* appears in the quadratic index of performance.

3) Observation and motor noise – Each variable observed by the pilot from his display is assumed to contain pilot-induced additive white noise, which scales with the variance of the observed variable. Each control output is assumed to contain pilot-induced additive white noise, which scales with the variance of the control.

4) Rate perception-If a variable is displayed explicitly, the pilot also perceives the first derivative of the variable, but no higher derivatives. The first derivative of the displayed variable also is noise-contaminated.

5) Index of performance – The index of performance for the optimization procedure is chosen subjectively by the analyst to mirror what he believes to be the task and control objectives as perceived by the pilot.

The placement of the pilot time delay at the control output constitutes the only major deviation from the model of Kleinman et al. Here, the delay is represented by a Padé approximation and is treated as part of the plant dynamics. The model of Ref. 4 subsumes the delay into the observation process. The only advantage afforded by the Padé approximation is that it allows direct use of existing computational algorithms for the solution of optimal estimation and control problems.

In what follows, a "displayed" variable will refer to a variable explicitly displayed to the pilot by the position of a display indicator. A "perceived" variable will refer to the time rate of change of a displayed variable. An "observed" variable will refer to either a displayed or perceived variable.

Figure 2 is a block diagram of the pilot-vehicle system. The equations that define the optimal pilot model follow.

System state equations

$$\dot{x}(t) = Ax(t) + Bu(t) + \gamma w(t)$$

$$E[w(t)w^T(t+\sigma)] = F\delta(\sigma) \tag{1}$$

where $x(t)$ represents the state, $u(t)$ the pilot's control output before his time delay and neuromuscular dynamics are encountered (see Fig. 2), and $w(t)$ represents white noise disturbances to be described. These equations include: 1) the vehicle dynamics; 2) the turbulence, represented by white noise with unity covariance passed through an appropriate shaping filter. The filter was chosen such that its output power spectral density was equivalent to that of the turbulence spectrum of Table 2; 3) the pilot's effective time delay, modeled as a first-order Pade approximation

$$e^{-\tau s} \doteq -(s-2/\tau)/(s+2/\tau) \tag{2}$$

4) the pilot's neuromuscular dynamics, modeled as a first-order lag

$$G(s) = 1/(T_N s + 1) \tag{3}$$

This lag is dynamically equivalent to including a weighting on control *rate* in the index of performance and adjusting the weighting coefficient on this term to yield a predetermined value of T_N[4]. In this study, the control rate term is not included in the index of performance, however; and 5) the motor noise, $v_m(t)$ which is white in nature, with covariance

$$E[v_m(t)\, v_m^T(t+\sigma)] = \rho' \pi E[u(t)\, u^T(t+\sigma)]\delta(\sigma) \tag{4}$$

Here ρ' is the predetermined noise-signal ratio for the motor noise.

Observation equations

$$z(t) = Hx(t) + v(t)$$

$$E[v(t)v^T(t+\sigma)] = G\delta(\sigma) \tag{5}$$

where $H\,x(t)$ represents the vector of variables displayed to or perceived by the pilot, and $v(t)$ is the vector of observation noises. The covariances of the individual observation noises

Table 3 Pilot model parameters for modeling of hover task

Time delay	τ	0.2 sec	
Neuromuscular time constant	T_N	0.2 sec	
Observation noise noise-signal ratio (full attention)	ρ	0.01	
Motor noise noise-signal ratio	ρ'	0.01	
Indifference thresholds	x_{TH}	0.305 m (1 ft)	0.00133 rad at pilot's eye
	$\dot{x}_{TH}$	0.914 m/sec (3 fps)	0.00399 rad/sec at pilot's eye
	h_{TH}	0.305 m (1 ft)	0.000667 rad at pilot's eye
	$\dot{h}_{TH}$	0.914 m/sec (3 fps)	0.00199 rad/sec at pilot's eye
	θ_{TH}	0.0175 rad	0.00166 rad at pilot's eye
	$\dot{\theta}_{TH}$	0.0525 rad/sec	0.005 rad/sec at pilot's eye
Q matrix coefficients			
	$q_{11}=1/\dot{x}_M^2$	$1/(0.305\ \text{m/sec})^2$	$[1/(1\ \text{ft/sec})^2]$
	$q_{22}=1/h_M^2$	$1/(7.62\ \text{m})^2$	$[1/(25\ \text{ft})^2]$
	$q_{33}=1/x_M^2$	$1/(3.05\ \text{m})^2$	$[1/(10\ \text{ft})^2]$
	$q_{44}=1/\dot{h}_M^2$	$1/(1.22\ \text{m/sec})^2$	$[1/(4\ \text{ft/sec})^2]$
R matrix coefficients			
	$r_{11}=1/u_{1_M}^2$	$1/(15.2\ \text{cm})^2$	$[1/(0.5\ \text{ft})^2]$
	$r_{22}=1/u_{2_M}^2$	$1/(15.2\ \text{cm})^2$	$[1/(0.5\ \text{ft})^2]$
Fractions of attention			
	f_t = fraction of attention on control task		=1.0
	f_s = fraction of attention on longitudinal subtask		=1.0
	f_1 = fraction of attention on pad displacement and rate		=0.333
	f_2 = fraction of attention on pitch attitude and rate		=0.333
	f_3 = fraction of attention on altitude and rate		=0.333

are

$$E[v_j(t)\ v_j(t+\sigma)] = \frac{\rho_j \pi E[z_j'(t)\ z_j'(t+\sigma)]\delta(\sigma)}{\hat{f}^2(z_j')} \tag{6}$$

where $z'(t)=Hx(t)$ and ρ_j is the noise-signal ratio associated with the jth displayed or perceived variable and $\hat{f}(z_j')$ is the amplitude dependent pure gain describing function for a threshold-type nonlinearity associated with the jth displayed or perceived variable.[5] This nonlinearity models pilot indifference thresholds on displayed or perceived variables.

Just as in Ref. 6, the effects of task interference were modeled as an increase in the nominal noise-signal ratios for each displayed variable. Thus

$$\rho_j = \rho \frac{1}{f_t}\frac{1}{f_s}\frac{1}{f_j} \tag{7}$$

where

ρ_j = noise-signal ratio associated with the jth observed quantity when attention is being shared

ρ = noise-signal ratio associated with "full attention" to the jth display

f_t = fraction of attention devoted to the control task as a whole

f_s = fraction of attention devoted to subtask s, e.g., longitudinal control

f_j = fraction of attention devoted to the jth observed quantity in subtask s, e.g., control of pitch attitude in the longitudinal subtask.

No task interference is assumed to occur between displayed and perceived variables, only between displayed variables.[7] Thus, a displayed quantity and its time derivative have the same ρ_j.

Index of performance

$$J = E\left\{\lim_{T\to\infty}\frac{1}{T}\int_0^T [y^T(t)Qy(t)+u^T(t)Ru(t)]\,dt\right\} \tag{8}$$

where $y(t)$ is given by

$$y(t)=Cx(t) \tag{9}$$

and $u(t)$ is the pilot's output before the effective time delay and neuromuscular dynamics are encountered.

B. Director Design Technique

The flight director design technique used here has its basis in the methods offered in Ref. 2. The method used here can be summarized as follows:

1) Given the vehicle/turbulence model and the baseline display, generate an optimal pilot model. The pertinent results of this analysis will be: a) predicted pilot transfer functions $h_{ij}(s)$ between each optimal control output $u_i(t)$ and each observed variable $z_j'(t)$; and b) the average power P_{ij} in each optimal control output $u_i(t)$, which is associated with each observed variable $z_j'(t)$.

2) Order each pilot transfer function $h_{ij}(s)$ calculated in item 1a according to the magnitude of the corresponding P_{ij} calculated in item 1b. Based upon this order, choose n_k "essential" observed variables for each control $u_i(t)$.

3) Formulate the flight director laws (one for each control) as follows.

$$d_i(s) = \sum_{j=1}^{n_k} h_{ij}(s)\ z_j'(s) \tag{10}$$

4) Since the a priori assumptions implicit in formulating the pilot model in item 1 may be in error, use simulation results to refine the model. With the refined model, repeat steps 1 through 3, and simulate again.

The method summarized in the preceding differs from that offered in Ref. 2 in two ways: 1) only "essential" variables are utilized in the director laws, and 2) the subject's neuromuscular dynamics are not included in the transfer functions used to describe the director laws.

The simplifications inherent in considering only the essential variables in the director design are obvious. Although the on-board sensing and computational capabilities of modern commercial or military aircraft probably would allow director laws utilizing complete feedback of pilot observed variables, the use of only essential feedbacks is highly desirable from the standpoint of director reliability and simplicity. In the case of general aviation aircraft, which normally lack sophisticated sensors or on-board computers, simplified director laws would be an absolute necessity. The exclusion of the subject's neuromuscular dynamics is consistent with the structure of the optimal pilot model. Specifically, the subject's physiological control-rate limitations are represented dynamically by a task-invariant first-order lag. Including the lag in the director law would be redundant, since the subject himself will generate the lag regardless of the form of the display compensation.

C. Model Specifics

For the UH-1H hover problem, Table 3 lists the model parameters chosen as the first step in the director design procedure. The parameters τ, T_N, and ρ are typical of values used in pilot-vehicle analyses using the optimal pilot model. The noise-signal ratio ρ' for the motor noise was chosen to be somewhat larger than the 0.003 value experimentally deter-

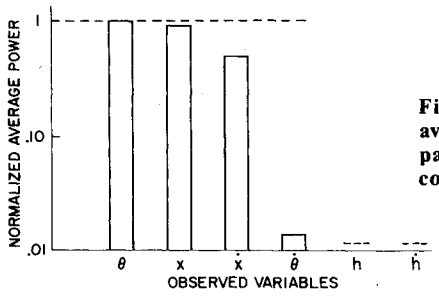

Fig. 3 Normalized average power comparisons for cyclic control.

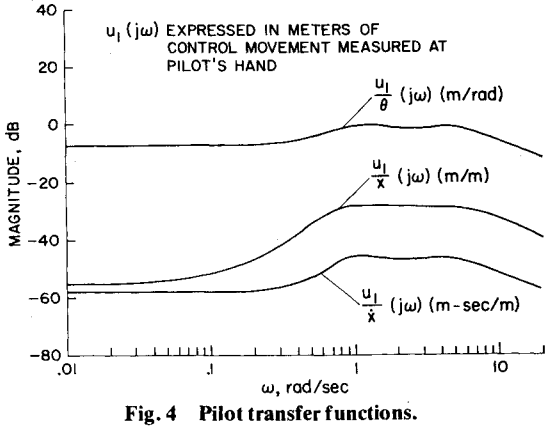

Fig. 4 Pilot transfer functions.

Table 4 Sinusoidal turbulence representation

$$u_g(t) = \sum_{k=1}^{5} A_k \sin\omega_k t$$

A_k, m/sec	ω_k, rad/sec
1.36	0.14
1.08	0.349
0.682	0.628
0.835	1.4
0.682	3.0

mined when an ideal manipulator was being used.[4] The indifference thresholds on the observed variables represent subjective estimates. The weighting coefficients in the index of performance are chosen as the reciprocals of "maximum allowable" deviations of the elements of ***y(t)*** and ***u(t)***. Such a selection scheme is suggested in Ref. 8 for optimal control problems in general, and is utilized in Ref. 6 for the optimal pilot model. The maximum allowable deviations also represent subjective estimates. The fractions of attention shown in the table imply that all of the pilot's attention is devoted to the control task, all of the control task attention is devoted to the longitudinal subtask, and ⅓ of the longitudinal subtask attention is devoted to each of the three displayed quantities (displacement from the pad center x, pitch attitude θ, and altitude deviation from the reference h). The f_t and f_s choices are logical in view of the longitudinal simulation, which is to follow. Normally, the f_j are chosen to minimize the index of performance and satisfy the constraints

$$\sum_{j=1}^{n} f_j = 1.0$$
$$f_j > 0 \quad j = 1,2,\ldots n \qquad (11)$$

where n is the number of displayed quantities. Although an efficient algorithm for solving for the optimum f_j recently has been developed,[9] it was assumed in this analysis that each of the three displayed quantities received equal attention. This was not a restrictive assumption since, in general, the index of performance is not a strong function of the f_j's.

D. Results

Figure 3 shows the normalized average power in the cyclic control due to the observed variables. Based upon this figure, the "essential" feedbacks were chosen as θ,x, and$\dot{x}$. Figure 4 shows the amplitude ratio portions of the Bode diagrams for the $u_l(s)/\theta(s)$, $u_l(s)/x(s)$, and $u_l(s)/\dot{x}(s)$ transfer functions. The model predicted virtually no collective motion; hence, no predicted transfer functions are shown. This lack of collective motion will be discussed later. The transfer functions shown in Fig. 4 were mechanized as simple lead-lag filters and were used to drive the cyclic director bar of Fig. 1 according to Eq. (10) in the simulation to be described. The display gain was 0.0833 cm of display movement per centimeter of commanded cyclic control (1 in./ft) measured at the pilot's hand.

III. Simulation

A. General Description

A simple, fixed-base pilot-in-the-loop simulation of the longitudinal task was conducted on the Naval Postgraduate School's hybrid computer. The vehicle dynamics were simulated on the analog computer, the displays were generated on a stroke-written CRT graphics terminal, with the digital computer driving the display elements. The nominal eye-to-display distance was 0.762 m (2.5 ft). The cyclic control device was a spring-restrained aircraft-type center-stick with a force-displacement gradient of 3.50 N/cm (2 lb/in.). The collective control was a device restrained only with an adjustable friction brake set to give a breakout force of 2.22 N (0.5 lb).

Four subjects were used in the experiment. All were helicopter pilots. Each subject flew the simulation with the display of Fig. 1 in a baseline and director configuration. Each run was of 90-sec duration. The turbulence of Table 2 was represented as the sum of five sine waves, whose amplitudes were chosen so that the frequency distribution of power closely matched that of the random turbulence. Table 4 shows this sinusoidal turbulence input.

B. Experimental Plan

The four test subjects had not flown in over a year, but had previously held instrument qualifications in helicopters. Prior to the beginning of each training session, all subjects were informed of the task requirements and familiarized with the operation of the simulator. The displays were shown and thoroughly explained. Because of the lack of recent flight time, it was felt that each subject would require considerable training until asymptotic performance levels were reached. This proved to be the case. The subjects were trained extensively on both the baseline and flight director displays. After each subject had reached his asymptotic performance level, data sessions were begun in which each subject completed ten runs with each display (baseline and director). The display configurations were altered, five runs with the baseline, five with the director, then five with the baseline, etc. The performance measures that were recorded were root mean square (rms) measures of longitudinal deviation from the pad center x, groundspeed deviation from hover $\dot{x}$, pitch attitude θ, pitch rate $\dot{\theta}$, height deviation from a reference datum h, time rate of change of height deviation $\dot{h}$, cycle control motion from trim δ_B, and collective control motion from trim δ_C. In addition, numerical pilot opinion ratings were elicited using the Cooper-Harper rating scale shown in Fig. 5.

C. Experimental Results

Table 5 lists the means and standard deviations of the measured rms performance scores for the baseline and direc-

CONTROLLABLE CAPABLE OF BEING CONTROLLED OR MANAGED IN CONTEXT OF MISSION, WITH AVAILABLE PILOT ATTENTION.	ACCEPTABLE MAY HAVE DEFICIENCIES WHICH WARRANT IMPROVEMENT, BUT ADEQUATE FOR MISSION. PILOT COMPENSATION, IF REQUIRED TO ACHIEVE ACCEPTABLE PERFORMANCE, IS FEASIBLE.	SATISFACTORY MEETS ALL REQUIREMENTS AND EXPECTATIONS, GOOD ENOUGH WITHOUT IMPROVEMENT. CLEARLY ADEQUATE FOR MISSION.	EXCELLENT, HIGHLY DESIRABLE.	A1
			GOOD, PLEASANT, WELL BEHAVED.	A2
			FAIR. SOME MILDLY UNPLEASANT CHARACTERISTICS. GOOD ENOUGH FOR MISSION WITHOUT IMPROVEMENT.	A3
		UNSATISFACTORY RELUCTANTLY ACCEPTABLE. DEFICIENCIES WHICH WARRANT IMPROVEMENT. PERFORMANCE ADEQUATE FOR MISSION WITH FEASIBLE PILOT COMPENSATION.	SOME MINOR BUT ANNOYING DEFICIENCIES. IMPROVEMENT IS REQUESTED. EFFECT ON PERFORMANCE IS EASILY COMPENSATED FOR BY PILOT.	A4
			MODERATELY OBJECTIONABLE DEFICIENCIES. IMPROVEMENT IS NEEDED. REASONABLE PERFORMANCE REQUIRES CONSIDERABLE PILOT COMPENSATION.	A5
			VERY OBJECTIONABLE DEFICIENCIES. MAJOR IMPROVEMENTS ARE NEEDED. REQUIRES BEST AVAILABLE PILOT COMPENSATION TO ACHIEVE ACCEPTABLE PERFORMANCE.	A6
	UNACCEPTABLE DEFICIENCIES WHICH REQUIRE MANDATORY IMPROVEMENT. INADEQUATE PERFORMANCE FOR MISSION EVEN WITH MAXIMUM FEASIBLE PILOT COMPENSATION.		MAJOR DEFICIENCIES WHICH REQUIRE MANDATORY IMPROVEMENT FOR ACCEPTANCE. CONTROLLABLE. PERFORMANCE INADEQUATE FOR MISSION, OR PILOT COMPENSATION REQUIRED FOR MINIMUM ACCEPTABLE PERFORMANCE IN MISSION IS TOO HIGH.	U7
			CONTROLLABLE WITH DIFFICULTY. REQUIRES SUBSTANTIAL PILOT SKILL AND ATTENTION TO RETAIN CONTROL AND CONTINUE MISSION.	U8
			MARGINALLY CONTROLLABLE IN MISSION. REQUIRES MAXIMUM AVAILABLE PILOT SKILL AND ATTENTION TO RETAIN CONTROL.	U9
UNCONTROLLABLE CONTROL WILL BE LOST DURING SOME PORTION OF MISSION.			UNCONTROLLABLE IN MISSION	10

Fig. 5 Revised Cooper-Harper scale.

tor configurations, along with the pilot ratings that each subject had given the configurations.

The differences in rms performance between the baseline and flight director configurations were substantial; rms position errors diminished by 16 to 45% longitudinally, and 17 to 39% vertically. The average Cooper-Harper rating for the baseline was A5.5, and for the director, A3.75. Pilot comments indicated that the flight director was definitely an aid in improving performance, and that it decreased pilot workload significantly.

IV. Model Refinement

A. Inducing Collective Motion

As pointed out in Sec. IIB, the a priori assumptions used in formulating the pilot model may be in error. In this example, the model predicted virtually no collective control motion, and very small height deviations and time rate of change of height deviations. The rms scores of Table 5 do not corroborate this prediction, and hence some refinement of the pilot model is necessary. In addition to this rather coarse model adjustment, the simulation performance results can be used to make finer model adjustments.

The lack of collective motion and vertical deviations in the modeling results can be explained as follows: With the horizontal turbulence primarily exciting the vehicle's horizontal translation and pitch attitude mode, the optimal control policy for the collective was essentially to keep the device at its still-air trim position. In reality, however, this trim position is never known precisely by the pilot. Off-nominal collective position excites the vertical translation model of the helicopter which the pilot then corrects with further collective motion, etc. One way to model this trim uncertainty is to incorporate a "residual" motor noise in the collective motion, i.e., a white

Table 5 Simulation rms performance scores

	Baseline				Preliminary director			
Subject:	1	2	3	4	1	2	3	4
x, m	1.94[a]	2.90	3.74	3.92	1.63	1.64	2.04	2.62
	0.378[b]	0.521	1.47	1.08	0.198	0.255	0.387	0.533
$\dot{x}$, m/sec	0.506	0.634	0.807	0.830	0.405	0.470	0.599	0.517
	0.079	0.103	0.244	0.152	0.061	0.042	0.125	0.0887
θ, rad	0.0284	0.0290	0.0354	0.0309	0.0242	0.0284	0.0349	0.0267
	0.00369	0.00573	0.0100	0.00501	0.00302	0.00268	0.00638	0.00413
$\dot{\theta}$, rad/sec	0.0193	0.0203	0.0223	0.0152	0.0146	0.0178	0.0224	0.0148
	0.00303	0.00429	0.00540	0.00298	0.00176	0.00206	0.00463	0.00235
h, m	2.18	2.25	3.50	3.32	1.81	1.82	2.12	2.04
	0.375	0.445	1.04	0.997	0.256	0.476	0.696	0.490
$\dot{h}$, m/sec	1.37	0.890	0.971	0.584	1.16	0.759	0.762	0.405
	0.283	0.187	0.238	0.208	0.110	0.180	0.187	0.109
δ_B, cm	1.16	1.27	1.33	0.901	0.863	1.07	1.36	0.914
	0.192	0.257	0.297	0.187	0.104	0.131	0.294	0.123
δ_C, cm	1.48	0.695	0.795	0.295	1.22	0.621	0.630	0.198
	0.406	0.156	0.256	0.120	0.133	0.191	0.129	0.0655
Cooper-Harper Ratings	A6	A6	A6	A4	A4	A5	A3	A3

[a] m-mean. [b] -variance.

noise that does not scale with the variance of the collective motion. Thus, the collective motor noise is given as

$$v'_{m_2}(t) = v_{m_2}(t) + r(t) \tag{12}$$

where $v_{m_2}(t)$ is the collective motor noise whose variance scales with the variance of $u_2(t)$, and $r(t)$ is the residual noise.

B. Model Specifics

In order to refine the pilot model, the rms performance data of subject 1 were used, and model parameters were adjusted so that model and simulation rms performance were in reasonable agreement. The data of subject 1 were chosen, since his rms performance was better on the whole than that of the other subjects.

The rule of thumb that was followed in adjusting the model parameters was to change as few parameters as little as possible from a priori values, so as to bring predicted rms scores into reasonable agreement with simulation scores. In the absence of describing function measurements, of course, rms performance scores are insufficient evidence of modeling accuracy.[10] However, as Ref. 11 points out, the number of measurable describing functions is equal to the number of uncorrelated disturbances (one in this case) times the number of pilot controls (two in this case). Thus, only two describing functions would be measurable in this simulation. Consequently, rms scores were relied upon for the purposes of comparison.

Table 6 indicates the model parameters that were altered from those of Table 3 in order to achieve reasonable rms performance comparisons. Note that the author altered only the magnitudes of the weighting coefficients in the index of performance, in addition to including residual motor noise. The flight director law for the cyclic control also was evaluated using the pilot model. Here, the covariance of the residual motor noise was lowered from that of the baseline configuration in order to achieve acceptable performance comparisons. In the director configuration, the observed quantities were assumed to be the director commands d_1 and d_2 and their time derivatives. As Table 6 indicates, the pilot was assumed to devote ½ of his longitudinal task attention to each of the two director commands. It should be noted that the weighting matrices in the index of performance were identical in the analyses of the baseline and director configurations, but the observed variables were different. Although the pilot was not assumed to use x and $\dot{x}$ for control in the director configurations, their inclusion in the index of performance is not unreasonable, since these variables can be monitored by the pilot while he used the observed variables d_1, d_2, $\dot{d}_1$, and $\dot{d}_2$ for control.

C. Comparison with Experimental Results

Figure 6 shows the comparison between experimental and model-generated rms performance scores. The comparison is reasonably good. The most serious model deficiency lies in the $\dot{h}$ predictions. Since the vertical translation mode is excited almost entirely by the residual motor noise, this modeling deficiency is not too surprising. For the purposes of this analysis, however, the model predictions were felt to be satisfactory.

D. Refined Pilot Transfer Functions

Since the director laws just discussed were obtained from a model with parameters chosen in a priori fashion, it would be of interest to determine analytically whether director laws obtained from the refined model would result in improved performance over the original director. Figure 7 shows the normalized average power in the cyclic and collective controls in the refined baseline model. Based upon this figure, the essential feedbacks were chosen as $x(t)$ and $\theta(t)$ for the cyclic, and $\dot{h}$ and $h(t)$ for the collective.

Table 6 Refined pilot model parameters

Q matrix coefficients[a]		
$q_{11} = 1/\dot{x}_M^2$	$1/(1.52\ \text{m/sec})^2$	$[1/(5\ \text{ft/sec})^2]$
$q_{22} = 1/h_M^2$	$1/(7.62\text{m})^2$	$[1/(25\ \text{ft})^2]$
$q_{33} = 1/x_M^2$	$1/(7.62\ \text{m})^2$	$[(1/25\ \text{ft})^2]$
$q_{44} = 1/\dot{h}_M^2$	$1/(3.05\ \text{m/sec})^2$	$[1/(10\ \text{ft/sec})^2]$
R matrix coefficients		
$r_{11} = 1/u_{1M}^2$	$1/(6.10\ \text{cm})^2$	$[1/(0.2\ \text{ft})^2]$
$r_{22} = 1/u_{2M}^2$	$1/(3.05\ \text{cm})^2$	$[1/(0.1\ \text{ft})^2]$
Covariance of collective residual motor noise		
$E[r^2(t)] = (1.0\ \text{cm})^2$	for baseline	
$(0.75\ \text{cm})^2$	for director	
Fractions of attention		
f_1 = fraction of attention on cyclic director command d_1	$=0.5$	
f_2 = fraction of attention on collective director command d_2	$=0.5$	

[a]The parameters shown in this table are the only refined model parameters which differ from those of Table 3.

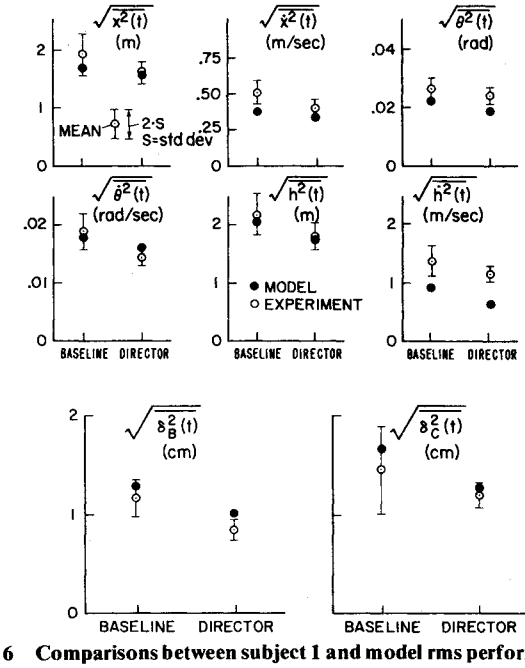

Fig. 6 Comparisons between subject 1 and model rms performance.

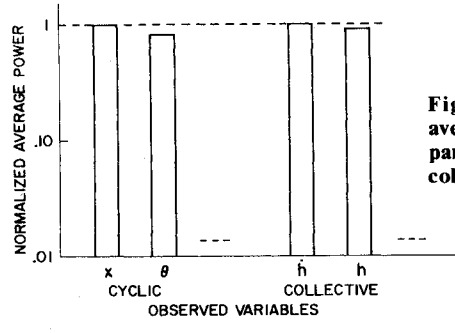

Fig. 7 Normalized average power comparisons for cyclic and collective controls.

Figure 8 shows the amplitude ratio portions of the Bode diagrams for the $u_1(s)/x(s)$, $u_1(s)/\theta(s)$, $u_2(s)/\dot{h}(s)$, and $u_2(s)/h(s)$ transfer functions. These transfer functions were used to derive director laws for cyclic *and* collective controls. The director gains used in the analysis were 0.417 cm of display movement per cm of commanded cyclic and collective

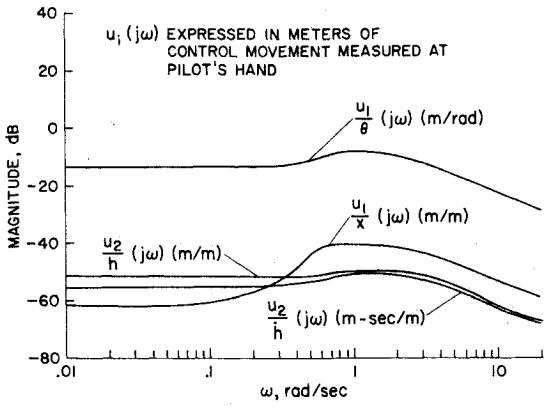

Fig. 8 Pilot transfer functions for revised model.

Table 7 Model rms performance scores

	Baseline	Preliminary director	Final director
x, m	1.70	1.55	0.90
$\dot{x}$, m/sec	0.39	0.33	0.21
θ, rad	0.022	0.019	0.013
$\dot{\theta}$, rad/sec	0.018	0.016	0.012
h, m	2.04	1.75	1.41
$\dot{h}$, m/sec	0.91	0.678	0.66
δ_B, cm	1.11	1.07	0.71
δ_C, cm	1.68	1.38	1.28

motion (5 in./ft). The director gains were chosen to be larger than those of Sec. II D, since predicted performance with the smaller gain was poor due to director threshold effects. The model parameters were identical to those of Table 6. Table 7 summarizes the model rms performance scores. The predicted performance improvements of the refined director are evident. No simulation study was conducted with the refined director laws, however.

V. Conclusions

Based upon the analytical and experimental study just discussed, the following conclusions can be drawn:

1) The model-based flight director design technique used here offers a straightforward procedure for determining director laws of minimum complexity. The computation of the normalized average power in each control due to each observed variable allows one to easily select "essential" variables for the director laws. The effectiveness of the director was demonstrated in the simulation where, even in the absence of a stability augmentation system, the director yielded significant improvements in performance and pilot acceptance.

2) Just as in the design technique of Ref. 2, the technique offered here should be considered as preliminary in nature, since factors such as wind shear and beam capture and noise have not been considered in the design process. In addition, the possibility of steady-state stand-off errors in which a steady-state value of one variable in the director law cancels the steady-state value of another variable should be considered in final implementation.

3) Although this paper discusses only longitudinal hovering flight, the technique can be applied to the design of directors for the complete approach and landing task, both lateral and longitudinal. The nominal approach and landing path ideally can be broken up into segments along which a time-stationary linear model can be applied. The resulting director laws for each discrete segment then can be joined smoothly to form a single, time-varying law for the entire task.

4) Simulation results are still invaluable in the design process. As demonstrated here, the experimental results allowed one to check the accuracy of the pilot model and refine the director laws.

5) The possibility of using this design technique to evaluate and modify fully automatic flight control systems should be investigated. Automatic systems that use significantly different control techniques than those that would be used by a pilot may well be deemed unacceptable by the pilot who must act as a system monitor for performance assessment or failure detection. In this light, the control techniques predicted by the model could be compared to those of proposed automatic flight control systems. If significant differences in control techniques are discovered, modifications of the automatic system could be considered.

References

[1]Weir, D.H., Klein, R.H., and McRuer, D.T., "Principles for the Design of Advanced Flight Director Systems Based on the Theory of Manual Control Displays," NASA CR-1748, March 1971.

[2]Levison, W.H., "A Model-Based Technique for the Design of Flight Directors," *Proceedings of the Ninth Annual Conference on Manual Control,* May 1973, pp. 163-172.

[3]Hess, R.A. and Wheat, L.W., "A Model-Based Analysis of a Display for Helicopter Landing Approach," *IEEE Transactions on Systems, Management and Cybernetics,* Vol. SMC-6, No. 7, July 1976, pp. 505-511.

[4]Kleinman, D.L., Baron, S., and Levison, W.H., "An Optimal Control Model of Human Response, Part I and II," *Automatica,* Vol. 6, May 1970, pp. 357-383.

[5]McRuer, D.T. and Graham, D., *Analysis of Nonlinear Control Systems,* John Wiley and Sons, New York, 1961, pp. 230-244.

[6]Baron, S. and Levison, W.H., "A Display Evaluation Methodology Applied to Vertical Situation Displays," *Proceedings of the Ninth Annual Conference on Manual Control,* May 1973, pp. 121-132.

[7]Levison, W.H., Elkind, J.I., and Ward, J.L., "Studies of Multivariable Manual Control Systems: A Model for Task Interference," NASA CR-1746, May 1971.

[8]Bryson, A.E. and Ho, Y.C., *Applied Optimal Control,* Blaisdell, Cambridge, Mass., 1969, p. 149.

[9]Curry, R.E., Kleinman, D.L., and Hoffman, W.C., "A Model for Simulataneous Monitoring and Control," *Proceedings of the Eleventh Annual Conference on Manual Control,* May 1975, pp. 144-150.

[10]Dey, D., "Problems, Questions and Results in the Use of the BBN-Model," *Proceedings of the Eleventh Annual Conference on Manual Control,* May 1975, pp. 577-598.

[11]Stapleford, R.L., McRuer, D.T., and Magdaleno, R., "Pilot Describing Function Measurements in a Multiloop Task," NASA CR-542, Aug. 1966.